Carbon Fibers Coated with Ternary Ni-Co-Se Alloy Particles as a Low-Cost Counter Electrode for Flexible Dye Sensitized Solar Cells

Carbon Fibers Coated with Ternary Ni–Co–Se Alloy Particles as a Low-Cost Counter Electrode for Flexible Dye Sensitized Solar Cells

Choudhury, Brishty[1], Lin, Che; Shawon[1], Sk Md Ali; Soliz-Martinez, Javier; Gutierrez, Jose; Huda, Muhammad[2]; Cesano, Federico [3]; Lozano, Karen[4]; Zhang, Jin[5]; Uddin, M.J. [1*]

[1] *Department of Chemistry, Photonic and Energy Research Laboratory, The University of Texas Rio Grande Valley, 1201 West University Dr, Edinburg, TX 78539, United States*

[2] *Department of Physics, The University of Texas at Arlington, Arlington, Texas 76019, United States;*

[3] *Department of Chemistry, University of Turin, Turin, TO, Italy*

[4] *Center for Nanotechnology, Department of Mechanical Engineering, The University of Texas Rio Grande Valley, Edinburg, Texas 78539, United States*

[5] *Department of Chemistry and Biochemistry, University of California, Santa Cruz, Santa Cruz, California 95064, United States*

* Corresponding Author Email: mohammed.uddin@utrgv.edu

Abstract

Compare to flat devices based on rigid substrates, fiber-shaped dye-sensitized solar cells hold advantages of smaller size, lightweight, facile fabrication, flexibility, and low cost, thus a promising direction for applications such as wearable electronic devices. However, most reported fiber-shaped dye-sensitized solar cells use Pt wires as counter electrodes, which make the applications suffer from high cost and scarcity. Herein, a flexible Pt-free counter electrode is fabricated via depositing ternary nickel cobalt selenide (Ni-Co-Se) particles on the surface of carbon fibers. Scanning electron microscopy and X-Ray diffraction are used to characterize the counter electrode and alloy material. Results from bare and modified carbon fiber counter electrodes reveal that Ni-Co-Se alloy particles greatly enhance electrocatalytic activity, leading to tremendous improvement in power conversion efficiency, which is comparable with devices using Pt wire counter electrode. Bending and multiple irradiation cycling tests are also performed to show the superior flexibility and durability of the novel device.

Keywords: *Ternary Co-Ni-Se alloy, Carbon fiber, Counter electrode, Dye-sensitized solar cells, Flexible.*

Introduction

Energy is an essential utility in the society. However, as traditional sources of energy, fossil fuels (coal, crude oil, and natural gas) are known to have harmful effects on environments and human health. Therefore, development of renewable/clean energy sources (i.e., solar, thermal, wind, nuclear fusion, etc.) attracts most attention in the energy field by far and is a popular research area. Among all the renewable/clean energy sources, because of sustainability, abundancy, and readily available in nature, solar energy is the most promising one. Therefore, tremendous efforts have been put into this research area over the past few decades to improve photovoltaic (PV) technologies such as dye sensitized, perovskite, and organic solar cells [1]. Compare to other PV techniques, dye-sensitized solar cells (DSSCs) developed since the late 1960s [2] have economic and simple fabrication processes, and high power conversion efficiencies (PCEs) [3-5]. However, planar structure DSSCs using rigid substrates are not compatible with applications where super flexibility is required, e.g. wearable electronic device. Fiber-shaped DSSCs (FDSSCs) are one type of PV device molded into a flexible fibrous structure, and they can be incorporated in broad range of important applications due to smaller size, lightweight, as well as ease in fabrication and low cost.

One general structure of a FDSSC has three major components: a photoanode, a counter electrode either arranged parallel to the photoanode or weaved around it, and an electrolyte with a pair of redox species. The most common photoanode consists of dye molecules loaded on a layer of TiO_2, which is stable, biologically and environmentally benign, inexpensive, and has excellent optical and electrical properties [6-9]. TiO_2 based photoanode has been widely studied and used in FDSSCs, because the material's appropriate electronic band structures allow the photon-excited electrons from dye molecules (usu. N719) be injected into the TiO_2 layer. Then the electrons are conducted to an external circuit to generate electric power and finally reach the counter electrode. The photo-oxidized dye molecules after electron injection can be restored by accepting electrons from the electrolyte, usually an organic solvent containing I^-/I_3^- redox pair. The reduced species can be subsequently regenerated at the surface of the counter electrode, by accepting the electron migrated through the external load. Overall, the device converts light energy to electric energy without permanently change the chemical composition of all components.

Though the photoanode plays the central role to generate electrons from light, the counter electrode is also critical in reforming the redox species. So far, many FDSSCs adopt Pt wire [10-15] or Pt based materials [16-17] as counter electrode, owing to high catalytic activity, chemical stability, and electrical conductivity [11,

[18-22]. However, high cost and rarity of Pt forbid its large-scale industrialized application. Hence, scientists have been working on developing Pt-free counter electrodes for FDSSCs. Among all the materials investigated, carbon-based counter electrodes are considered ideal for fiber shaped devices, as they are highly conductive, mechanically robust, lightly weighted, low cost, and very flexible. On the other hand, major shortcomings of carbon-based counter electrodes include slow charge transfer rate and limited ability for electrocatalysis of bare carbon materials. Researchers in this area have been working to solve these challenges. For example, L. Chen et. al. reported a FDSSC with TiO_2 nanotube arrays in the photoanode and bare carbon fiber (CF) as counter electrode had a power conversion efficiency (PCE) of 1.03%; when the bare CF was coated with $CoNi_2S_4$ nanorod or $CoNi_2S_4$ nanoribbon, PCE of devices dramatically improved to 4.10 % and 7.03%, respectively [23]. Z. Yang et. al. fabricated FDSSC with PCE 7.13%, and the counter electrode used was made with multiwall carbon nanotubes (MWCNTs) array [24]. In the work conducted by T. Chen et. al., the device had aligned titania nanotubes as a photoanode material, and aligned carbon nanotube (CNT) fibers in counter electrode (CE); the resulted PCE was 2.20% [25]. A. Ali et. al. showed that MWCNT coated with poly (3,4-ethylene dioxythiophene):poly(styrene sulfonate) reached PCE of 5.03% [26]. The highest PCE achieved by far based on Pt-free counter electrode (10.28%) was done by J. Zhang et. al.; their group used $Co_{0.85}Se$ nanosheets on the polyaniline functionalized CFs [27].

In the above-mentioned examples, higher PCE of the device could be achieved by coating a conductive polymer layer on the carbon-based counter electrode [26-27], and/or using transition metal chalcogenides [23, 27]. The latter method attracts attention because these materials are resistant to electrolyte corrosion, active for I_3^- reduction, and also inexpensive [28-29]. In L. Chen's article [23], ternary $CoNi_2S_4$ was used, as the device could take advantage of both cobalt and nickel ions, which could provide richer redox reactions than binary CoS or NiS. J. Zhang et. al. reported use of $Co_{0.85}Se$ [27], as metal selenides are known to have distinctive chemical and electronic properties, therefore great potential for a broad range of applications [30-32]. In the work of L. Shao et. al. [33], hollow microspheres based on ternary nickel cobalt selenide (Ni-Co-Se) alloy were synthesized via a simple one-step hydrothermal route, and the corresponding flat cell using this material in the CE had PCE up to 9.04% and higher than cells with Pt CE (8.07%).

In this work, we report synthesis and properties of Ni-Co-Se particles, and of the same ternary metal selenides attached to CF to form Pt-free fiber shaped CEs. Performances of devices with Ni-Co-Se synthesized at different temperatures, as well as FDSSCs with Pt CE, and bare CF CE, are compared. The

FDSSCs based on the Ni-Co-Se on carbon fiber (Ni-Co-Se@CF) counter electrode achieved the highest power conversion efficiency of 2.01%, comparable with CF CEs or CF CEs coated with Pt. In addition, the fabricated FDSSCs show good flexibility.

Experimental Section

Preparation of photoanode

For photoanode preparation several Ti wires (φ = 250 μm) were cleaned by ultrasonicating in ethanol, acetone, and propanol for 15 minutes subsequently. After that, a NaOH solution of 2.5 M has been prepared. 30 mL of this NaOH solution has been put into a Teflon-lined stainless-steel autoclave and the cleaned Ti wires have been immersed into the solution. The reactor was subsequently placed into a furnace at 220°C for 15-24 hours. After, the reactor was cooled down to room temperature and the wires were washed thoroughly with acetone. Then the wires were put into a 1 M HCl solution for 1 hour. The wires were then again washed thoroughly with acetone to get Ti wire with TiO_2 nanowires (NWs). These Ti wires with TiO_2 NWs were used as the photoanode.

Preparation of Co-Ni-Se Hollow Microspheres

0.757g of $Co(NO_3)_26H_2O$ [Cobalt(II) Nitrate Hexahydrate], 0.378g of $Ni(NO_3)_26H_2O$ [Nickel(II) Nitrate Hexahydrate] (Ni:Co = 1:2), and 2.6mL of Ethylenediamine was dissolved in 40 mL of distilled water. 0.692g of Na_2SeO_3 [Sodium Selenite] (Ni:Co:Se = 1:2:4) was added to this solution. After an ultrasonic bath for 20 mins, the mixed solution was put in a Teflon-lined stainless-steel autoclave reactor. The reactor was put in an electric oven at different temperatures (i.e. 140°C, 160°C, 180°C, 200°) for 24 hours. After that, the reactor was cooled down to room temperature and the precipitate was centrifuged. The precipitate was washed thoroughly with absolute ethanol several times. The precipitate was then dried in an electrical oven at 80°C for 12 hours. The dried products were labeled as Ni-Co-Se-140, Ni-Co-Se-160, Ni-Co-Se-180, and Ni-Co-Se-200.

Preparation of Counter Electrode

Commercial carbon fiber tow has been used as the substrate. Before using the carbon fibers (CFs), they have been treated through several treatments to increase their conductivity. First the CF yarn was soaked in acetone for 3 hours to remove any polymer coating present on the surface. Then the CF yarn was washed with milli-Q water, acetone, ethanol respectively under light sonication. Then the CF was kept into a tube

furnace at 300°C for 2 hours under light airflow to thermally degrade the polymer coating. Then the fiber yarn was again washed with milli-Q water, acetone, ethanol respectively under light sonication. The fiber was subsequently kept into a 70% HNO_3 solution under mild stirring for 12 hours. The fiber was again washed with milli-Q water, acetone, ethanol respectively under light sonication. After drying, the CF yarn was cut into pieces of length 6-7 cm. 5 mg of the Ni-Co-Se sample was dispersed into 2-5 mL of water. The mixed solution was ultrasonically treated to make a uniform dispersion. The CFs were then dipped coated using this solution and labeled as CF-140, CF-160, CF-180, -CF-200. To make the comparison, a carbon fiber was also coated with Pt using a plasma sputtering system.

Fabrication of FDSSC

The photoanodes prepared on Ti wire were soaked into 0.5 mM N719 dye solution (a solvent mixture of acetonitrile and tert-butyl alcohol in a volume ratio of 1:1) for 24 hours. After that, the photoanodes were washed with acetonitrile to remove excess dye. The different CEs were wrapped around the photoanodes. The assembly was inserted into a glass capillary and an electrolyte was injected into the capillary. The electrolyte was prepared by dissolving 0.5 M LiI, 0.05 M I_2, and 0.5 M tert-butyl pyridine and brought up to 10 ml volume in 3-methoxy propionitrile. 5 wt% poly (vinylidene fluoride-co-hexafluoropropylene) was added to this solution. The mixed solution was dissolved overnight with mild heating and vigorous stirring to make a homogeneous solution.

Morphological, structural and Photovoltaic Characterizations: The morphological characterization has been done using scanning electron microscopy (SEM, EVO LS10 STEM). X-ray diffraction (XRD) measurements were conducted using a "BRUKER™ D8 X-ray Diffractometer" with a Cu $K\alpha_1$ radiation (λ = 0.15406 nm, 40 kV, 40 mA). The scanning mode was set to 2θ, and the scanning range was from 10° to 90° with a scanning step size of 0.04° and scanning rate of 1.0° min^{-1}. The photocurrent-voltage measurements were carried out using a VersaSTAT3 potentiostat (Princeton Applied Research) running cyclic voltammetry with a scan rate of 50 $mV \cdot s^{-1}$. A Honle solar simulator 400, with an AM 1.5G spectrum (100 mW/cm^2) was used to simulate sunlight for irradiating the cells.

Result and Discussion

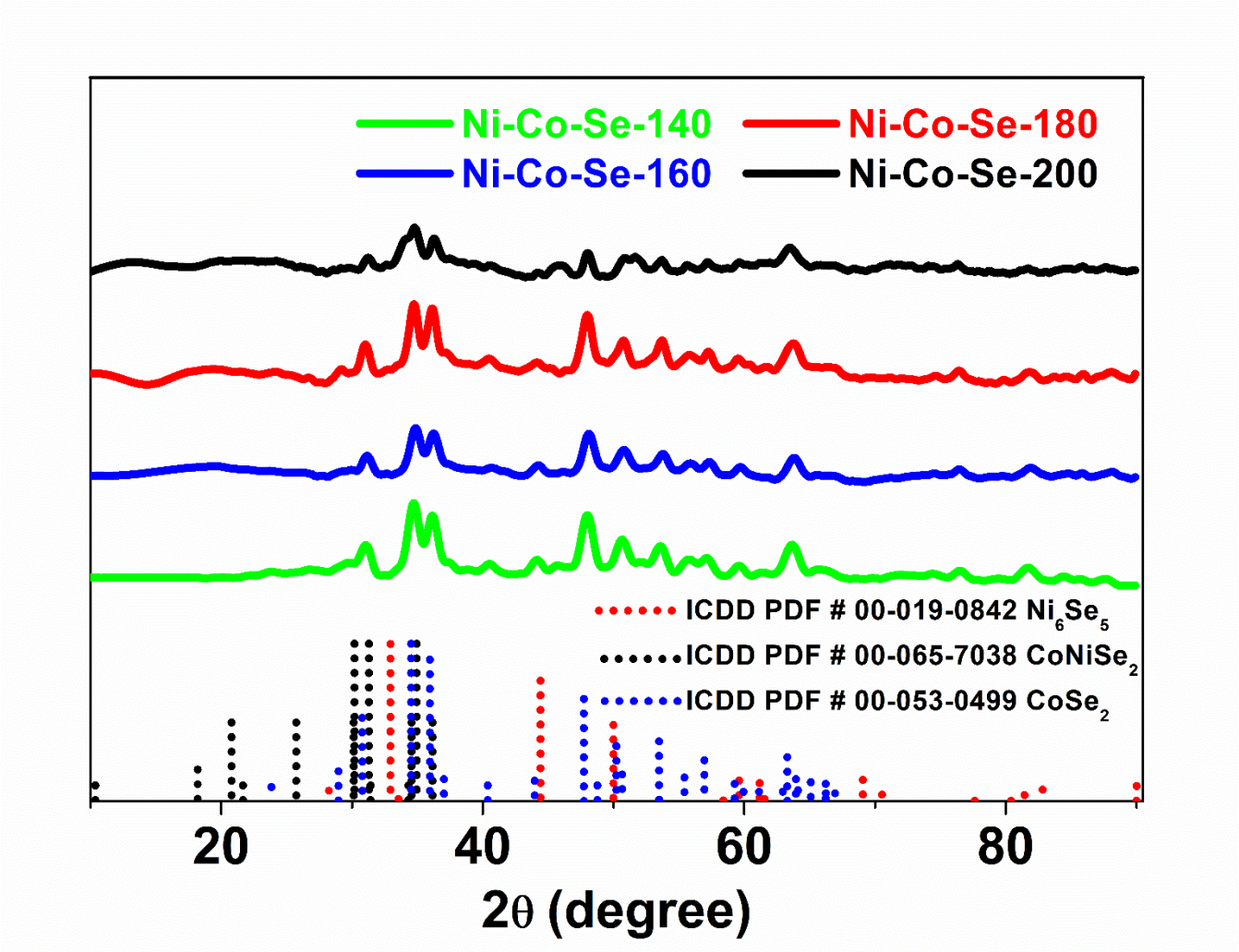

Figure 1: XRD patterns of the samples Ni-Co-Se-140, Ni-Co-Se-160, Ni-Co-Se-180, Ni-Co-Se-200. XRD peak positions for Ni_6Se, $CoNiSe_2$ and $CoSe_2$ are also present for the comparison.

Figure 1 shows the XRD patterns of the Ni-Co-Se alloys synthesized at different hydrothermal reaction temperature. It is evident that all the samples show XRD patterns with very similar peaks. Such peaks can be successfully assigned to the orthorhombic $CoSe_2$ (JCPDS PDF no. 00-053-0499) and in a small extent to orthorhombic Ni_6Se_5 (JCPDS PDF no. 00-019-0842). Apart from these peaks, no other features are present in the patterns. The well-defined peaks that appear at $2\theta = 34.7°, 36.2°, 40.5°, 44.1°, 48.0°, 50.8°,$

53.5°, and 63.5° corresponds to orthorhombic $CoSe_2$ (111), (120), (210), (121), (211), (002), (031), and (122) crystal planes, respectively. These values agree with the previous report[33]. The peaks at $2\theta \cong 31.0°$, 35.1°, 36.9° corresponds to the crystal planes of orthorhombic Ni_6Se_5 (040), (025), (113), respectively. In case of Ni-Co-Se-160 another set of peaks is found in the pattern which can be successfully assigned to the hexagonal $CoNiSe_2$ (JCPDS PDF no. 00-065-7038). The peaks at $2\theta \cong 44.4°$ and 50.0°corresponds to (102) and (110) planes, respectively. So, the XRD patterns of the synthesized alloy should contain only the orthorhombic crystal structure except for the Ni-Co-Se-160 which should contain an additional hexagonal crystal structure. It looks like the temperature does not have a significant effect on the crystal structure. However, in case of Ni-Co-Se-200 the peaks intensity seems like to reduce slightly, which implies that increased temperature reduces crystallinity.

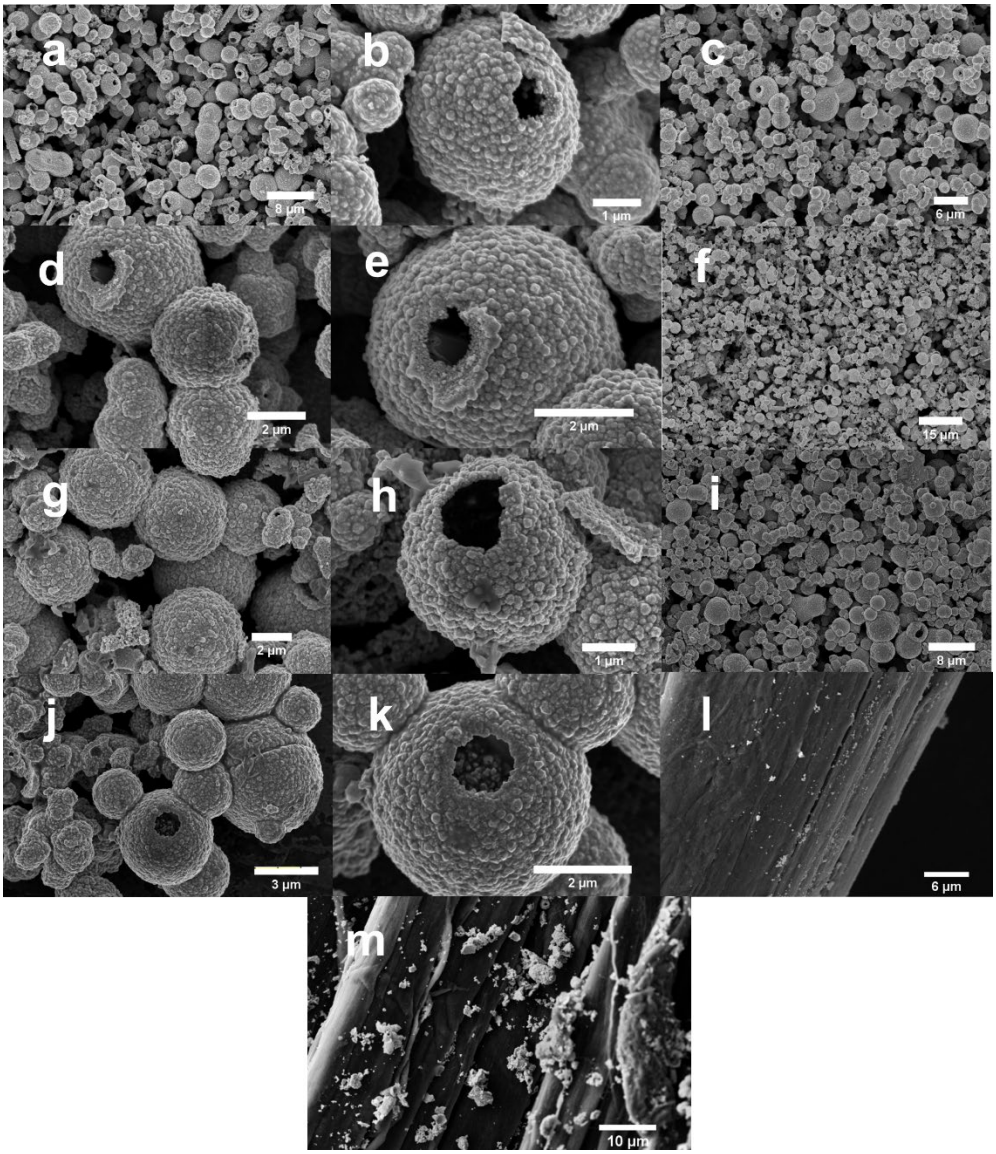

Figure 2: SEM images of Ni-Co-Se synthesized at different hydrothermal reaction temperature, (a,b) Ni-Co-Se-140, (c-e) Ni-Co-Se-160, (f-h) Ni-Co-Se-180, (i-k) Ni-Co-Se-200, (l) CF, (m) CF coated with Ni-Co-Se alloy.

The structural morphologies of the alloys have been done by taking SEM image of the samples prepared at different hydrothermal reaction temperatures. In **Figure 2 a, c, f, i** SEM images of the synthesized alloy in bulk are shown. **Figure 2 a** reveals that apart from the spherical hollow microspheres there are still a significant number of stick-like hollow alloy structures. However, the formation of spherical alloys increases with increasing temperature. While looking at individual microspheres they seem not to affect much by the different hydrothermal reaction temperatures. The surface of the microspheres seems rough due to the crosslinked nanoparticles and no smooth surface is visible in the SEM images. The microspheres again connect with each other forming a network. Some irregular structures are also visible which implies the formation of microspheres was incomplete in those locations. The stability of the microspheres at different hydrothermal reaction temperature is very much evident, as no broken or honeycomblike structures are present. **Figure 2 (l)** shows a portion of bare CF which slightly rough surface, which is suitable for the deposition of the Ni-Co-Se alloy. The CFs were filament initially. While making counter electrode they have been twisted to make then thin fibre-like structure. The roughness appears due to the twisting of the filament. **Figure 2 (m)** shows the successful anchoring of the alloys on the CF yarn.

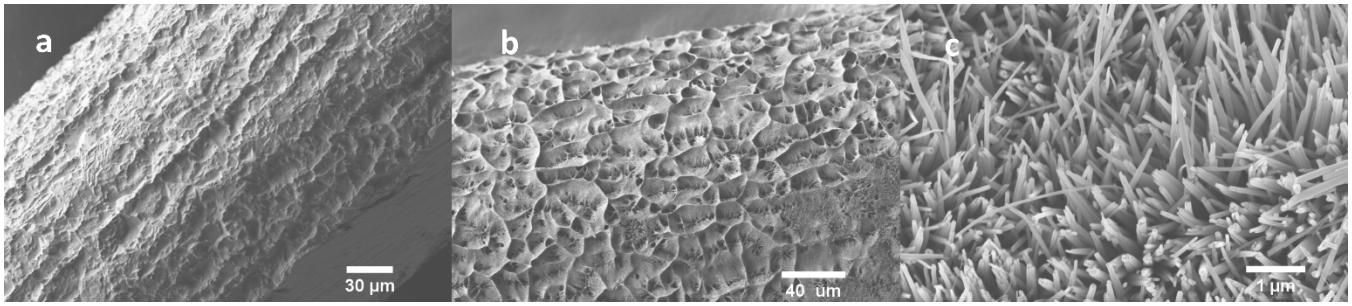

Figure 3: (a) Bare Ti wire, (b) Ti wire coated with TiO_2 NWs, (c) zoomed view of individual NWs

Figure 3 shows the SEM image of photoanode. Figure 3 a shows bare surface of Ti wire before the NW growth. The Ti wire reacts with NaOH to form $Na_2Ti_2O_5 \cdot 3H_2O$ which after the HCl treatment converts to $TiO_2(H_2O)_5$. The annealing treatment removes the water molecules to eventually yield TiO_2 NWs[34]. From

Figure 3- b and **c,** it can be seen that the Ti thread is uniformly covered with TiO_2 NWs, which are grown and radially oriented and protruding from the Ti wire. TiO_2 NWs are 1-4 µm in length and have diameters of 100-250nm. It is worthy noticing that the elongated structure of the NWs can facilitate the electron transport

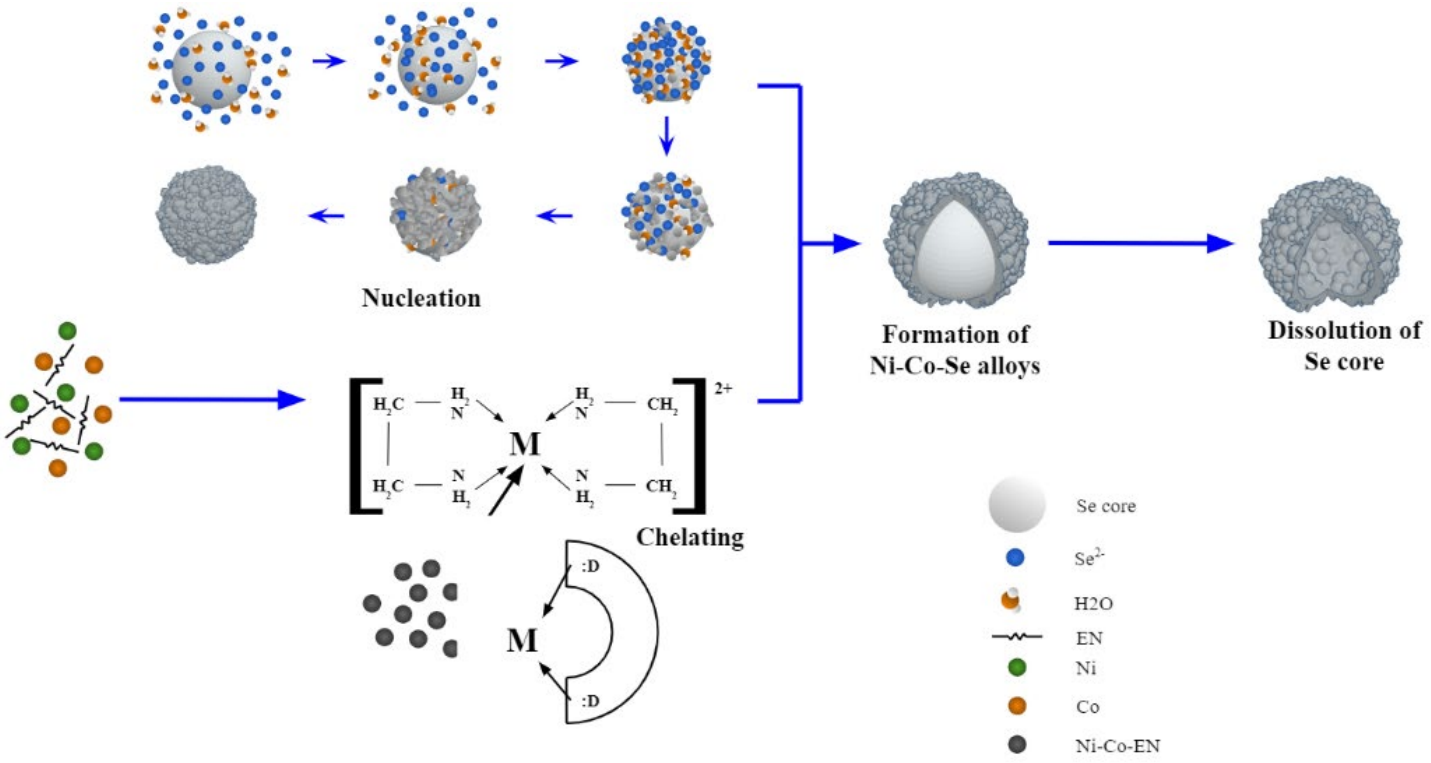

Figure 4: Formation mechanism of Ni-Co-Se hollow microspheres.

The Formation Mechanism for the Ni-Co-Se Hollow Microspheres

Based on the above observations and studying the previous literature the formation mechanism of Ni-Co-Se hollow microspheres can be proposed in the following way. Ethylenediamine (EDA) plays a significant role in the formation of final desired product (Figure 4). As EDA possesses $-NH_2$ functional groups at both ends, it acts as a powerful chelating agent. It forms a stable chelating complexes by forming bonds with Ni^{2+} and Co^{2+} ions as is also evident from the change of color of the reaction mixture from pale red to dark brown[35]. EDA also plays an important role in determining the surface morphology of the final product by controlling the hollow microsphere growth[36-37]. After forming the chelating complex, it can control the release rate of Ni and Co ions from the complex and thus improves the hollow microsphere morphology by lowering the Ni-Co-Se powder generation. Sodium selenite acts as the Se source in this

reaction and gets reduced by Co^{2+} or EDA to form Se core, which is also evident during the experiment as the gray Se powder is produced immediately upon adding sodium selenite in the solution[37]. The bimetallic chelates containing the Ni and Co ions get attached to Se core. A further reaction occurs through the mutual diffusion of the Se core and the chelating complex to form Ni-Co-Se particles. Subsequently, a bridged structure is formed and through around the Se core with reaction temperature increasing. As a result of this process, the Se core disappears and the hollow Ni-Co-Se microspheres are formed. This in situ nucleation involves a growth-driven force for the formation of the hollow microspheres[38-41]. During the process, the Se^{2-} in the solution also bonds with the atoms on the growing Se core by van der Waals. However, this force is weak compared to the electrostatic attraction between the polar water molecule and Se^{2-} ions. As a result, once the Se^{2-} ions bond to the Se core they are pulled back instantly to the solution. Hence, the surface of the product Ni-Co-Se hollow microspheres appear rough.

Photovoltaic Characterization

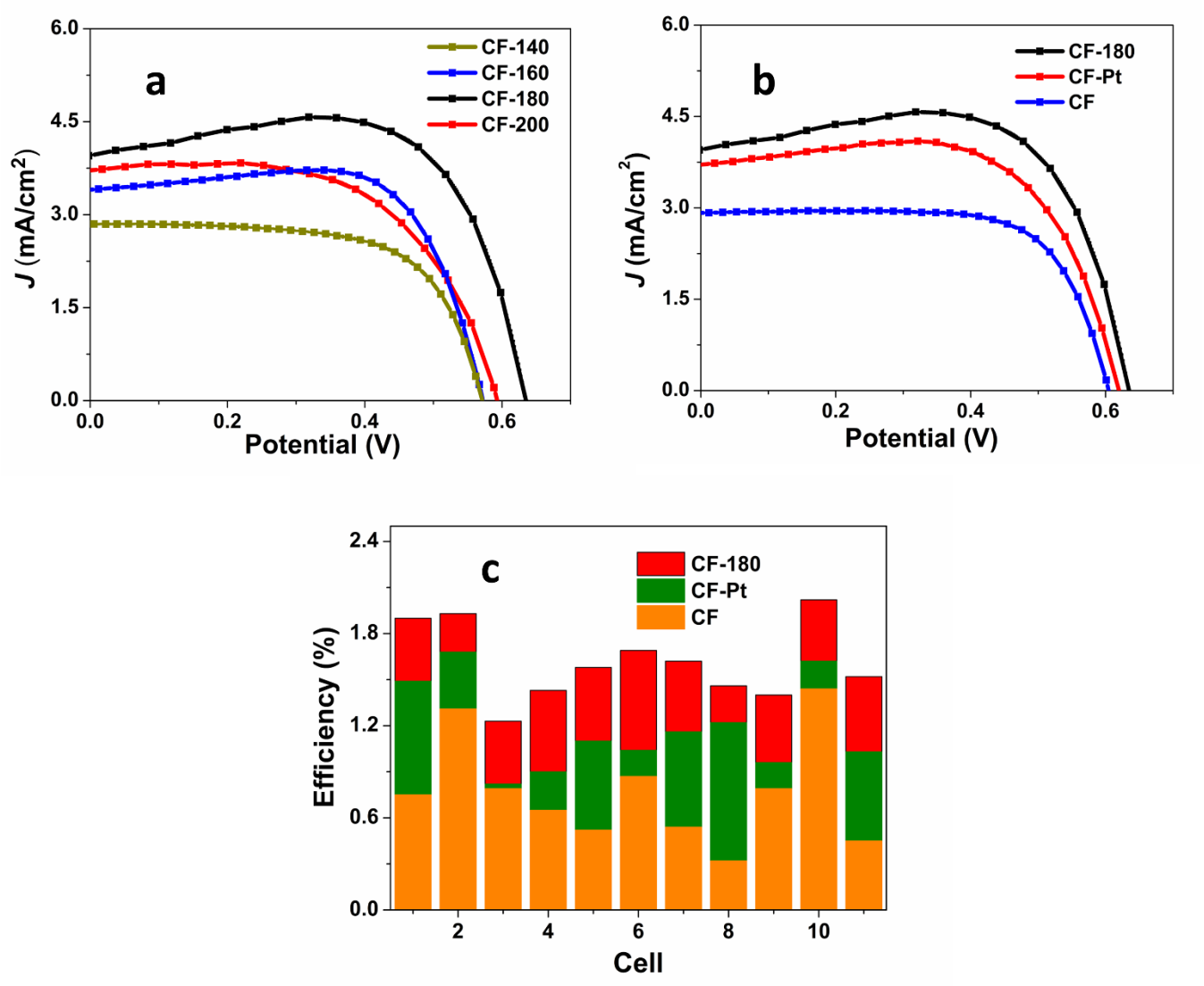

Figure 5: a) comparison of *J-V* plot between CF-140, CF-160, CF-180, and CF-200, b) comparison of *J-V* plot between CF-180, CF-Pt, and CF, c) a performance analysis of CF-180, CF-Pt, and CF based on 11 cells using each of the CE.

Figure 5-a, b represents the photovoltaic performance of the counter electrodes coated with different types of hollow microsphere alloys. As the hydrothermal temperature increases both the J_{sc} and V_{oc} keeps increasing and the after 180°C, the performance again drops. The reason can be attributed to the fact that, with increased hydrothermal reaction time, the hollow microsphere growth is achieved perfectly, and the crystallinity also increases. At lower hydrothermal reaction, the hollow sphere growth is incomplete, leading to a lot of hollow sticklike structures. The best performance of the CE has been found for a

hydrothermal reaction of 180°C. Apart from the successful formation of the hollow microspheres the other reason can be attributed to the efficient reduction of the I_3^- to I^-.

Table 1: Photovoltaic properties of FDSSC using different CEs.

CE	J_{sc}, mA/cm^2	V_{oc}, Volt	Efficiency, %	FF
CF-140	2.83	0.57	1.08	0.67
CF-160	3.76	0.59	1.41	0.62
CF-180	3.96	0.63	2.03	0.53
CF-200	3.39	0.57	1.51	0.8
CF-Pt	3.68	0.62	1.69	0.74
CF	2.88	0.6	1.27	0.73

To test the flexibility and photostability of the devices, the performance of the cells after bending under severe conditions (180°) 10 times and after illuminating for multiple radiation cycles has been performed (Figure 6a,b). In both cases, the devices significantly retain their performance. The reason can be attributed to the good adhesion between the hollow microspheres and the CF, to the increased smoothness and properties of the carbon fibers, which are flexible in nature and possess excellent stability against corrosion by I_3^-/I^- electrolyte.

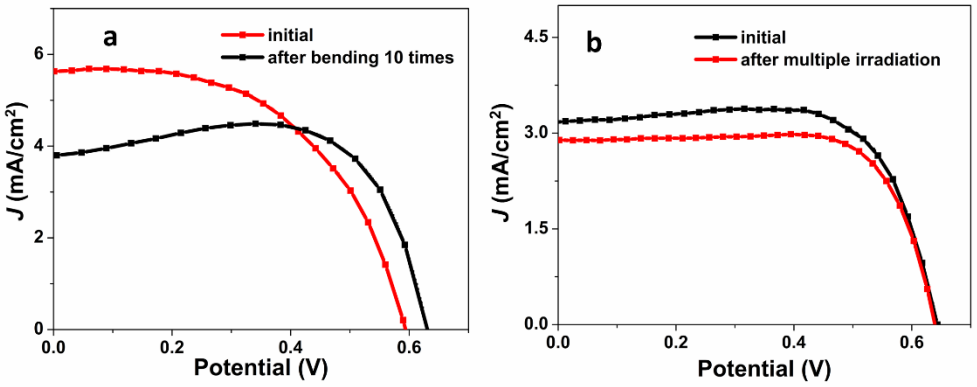

Figure 6: a) comparison of performance after bending 10 times c) comparison of performance after irradiating the cell for 10 times.

Conclusion

In summary, ternary Ni-Co-Se hollow microspheres based on platinum-free electro-catalyst has been synthesized and its photovoltaic performance has been evaluated. The shape of such ternary microspheres is strongly dependent on the hydrothermal reaction temperature, which plays a critical role to determine the crystallinity of the samples. The XRD analysis confirms the successful formation of the desired composition. The SEM analysis ensures the morphology of the alloys to be hollow microspheres. When compared with CE consisting of CF coated with Pt, and bare CF, a significant increase in the light-to-current conversion efficiency has been achieved for the nanostructured Ni-Co-Se systems attached on the surface of carbon fiber yarn working as counter electrode in a fiber-shaped DSSC. To test the flexibility of the device the cells were bent to 180 ° for 10 times and the J-V data were taken, which shows the cells retain their performance significantly. Also, the cells retain their performance under multiple times of irradiation.

1. Hatamvand, M.; Kamrani, E.; Lira-Cantu, M.; Madsen, M.; Patil, B. R.; Vivo, P.; Mehmood, M. S.; Numan, A.; Ahmed, I.; Zhan, Y. Q., Recent advances in fiber-shaped and planar-shaped textile solar cells. *Nano Energy* **2020,** *71*, 17.
2. Gerische.H; Michelbe.Me; Rebentro.F; Tributsc.H, SENSITIZATION OF CHARGE INJECTION INTO SEMICONDUCTORS WITH LARGE BAND GAP. *Electrochim. Acta* **1968,** *13* (6), 1509-&.
3. Oregan, B.; Gratzel, M., A LOW-COST, HIGH-EFFICIENCY SOLAR-CELL BASED ON DYE-SENSITIZED COLLOIDAL TIO2 FILMS. *Nature* **1991,** *353* (6346), 737-740.
4. Gratzel, M., Photoelectrochemical cells. *Nature* **2001,** *414* (6861), 338-344.
5. Yella, A.; Lee, H. W.; Tsao, H. N.; Yi, C. Y.; Chandiran, A. K.; Nazeeruddin, M. K.; Diau, E. W. G.; Yeh, C. Y.; Zakeeruddin, S. M.; Gratzel, M., Porphyrin-Sensitized Solar Cells with Cobalt (II/III)-Based Redox Electrolyte Exceed 12 Percent Efficiency. *Science* **2011,** *334* (6056), 629-634.
6. Chen, X.; Mao, S. S., Titanium dioxide nanomaterials: Synthesis, properties, modifications, and applications. *Chem. Rev.* **2007,** *107* (7), 2891-2959.
7. Li, W.; Wu, Z. X.; Wang, J. X.; Elzatahry, A. A.; Zhao, D. Y., A Perspective on Mesoporous TiO2 Materials. *Chem. Mat.* **2014,** *26* (1), 287-298.
8. Wold, A., PHOTOCATALYTIC PROPERTIES OF TIO2. *Chem. Mat.* **1993,** *5* (3), 280-283.
9. Wu, H. B.; Hng, H. H.; Lou, X. W., Direct Synthesis of Anatase TiO2 Nanowires with Enhanced Photocatalytic Activity. *Adv. Mater.* **2012,** *24* (19), 2567-2571.
10. Pu, X.; Song, W. X.; Liu, M. M.; Sun, C. W.; Du, C. H.; Jiang, C. Y.; Huang, X.; Zou, D. C.; Hu, W. G.; Wang, Z. L., Wearable Power-Textiles by Integrating Fabric Triboelectric Nanogenerators and Fiber-Shaped Dye-Sensitized Solar Cells. *Adv. Energy Mater.* **2016,** *6* (20), 9.
11. Liu, G. C.; Wang, M. X.; Wang, H.; Ardhi, R. E. A.; Yu, H. J.; Zou, D. C.; Lee, J. K., Hierarchically structured photoanode with enhanced charge collection and light harvesting abilities for fiber-shaped dye-sensitized solar cells. *Nano Energy* **2018,** *49*, 95-102.

12. Liu, G. C.; Wang, H.; Wang, M. X.; Liu, W. B.; Ardhi, R. E. A.; Zou, D. C.; Lee, J. K., Study on a stretchable, fiber-shaped, and TiO2 nanowire array-based dye-sensitized solar cell with electrochemical impedance spectroscopy method. *Electrochim. Acta* **2018,** *267*, 34-40.
13. Li, Z. D.; Zhou, Y.; Yang, Y. H.; Dai, H., Electrophoretic deposition of graphene-TiO2 hierarchical spheres onto Ti thread for flexible fiber-shaped dye-sensitized solar cells. *Mater. Des.* **2016,** *105*, 352-358.
14. Peng, M.; Yan, K.; Hu, H. W.; Shen, D. H.; Song, W. X.; Zou, D. C., Efficient fiber shaped zinc bromide batteries and dye sensitized solar cells for flexible power sources. *J. Mater. Chem. C* **2015,** *3* (10), 2157-2165.
15. Peng, M.; Dong, B.; Cai, X.; Wang, W.; Jiang, X. M.; Wang, Y. H.; Yang, Y.; Zou, D. C., Organic dye-sensitized photovoltaic fibers. *Sol. Energy* **2017,** *150*, 161-165.
16. Wen, Z.; Yeh, M. H.; Guo, H. Y.; Wang, J.; Zi, Y. L.; Xu, W. D.; Deng, J. N.; Zhu, L.; Wang, X.; Hu, C. G.; Zhu, L. P.; Sun, X. H.; Wang, Z. L., Self-powered textile for wearable electronics by hybridizing fiber-shaped nanogenerators, solar cells, and supercapacitors. *Sci. Adv.* **2016,** *2* (10), 8.
17. Fu, X. M.; Sun, H.; Xie, S. L.; Zhang, J.; Pan, Z. Y.; Liao, M.; Xu, L. M.; Li, Z.; Wang, B. J.; Sun, X. M.; Peng, H. S., A fiber-shaped solar cell showing a record power conversion efficiency of 10%. *J. Mater. Chem. A* **2018,** *6* (1), 45-51.
18. Liu, G. C.; Peng, M.; Song, W. X.; Wang, H.; Zou, D. C., An 8.07% efficient fiber dye-sensitized solar cell based on a TiO2 micron-core array and multilayer structure photoanode. *Nano Energy* **2015,** *11*, 341-347.
19. Lv, Z. B.; Yu, J. F.; Wu, H. W.; Shang, J.; Wang, D.; Hou, S. C.; Fu, Y. P.; Wu, K.; Zou, D. C., Highly efficient and completely flexible fiber-shaped dye-sensitized solar cell based on TiO2 nanotube array. *Nanoscale* **2012,** *4* (4), 1248-1253.
20. Liu, G. C.; Gao, X.; Wang, H.; Kim, A. Y.; Zhao, Z. X.; Lee, J. K.; Zou, D. C., A novel photoanode with high flexibility for fiber-shaped dye sensitized solar cells. *J. Mater. Chem. A* **2016,** *4* (16), 5925-5931.
21. Song, W. X.; Wang, H.; Liu, G. C.; Peng, M.; Zou, D. C., Improving the photovoltaic performance and flexibility of fiber-shaped dye-sensitized solar cells with atomic layer deposition. *Nano Energy* **2016,** *19*, 1-7.
22. Tao, H.; Fang, G. J.; Ke, W. J.; Zeng, W.; Wang, J., In-situ synthesis of TiO2 network nanoporous structure on Ti wire substrate and its application in fiber dye sensitized solar cells. *J. Power Sources* **2014,** *245*, 59-65.
23. Chen, L.; Zhou, Y.; Dai, H.; Yu, T.; Liu, J. G.; Zou, Z. G., One-step growth of CoNi2S4 nanoribbons on carbon fibers as platinum-free counter electrodes for fiber-shaped dye-sensitized solar cells with high performance: Polymorph-dependent conversion efficiency. *Nano Energy* **2015,** *11*, 697-703.
24. Yang, Z. B.; Deng, J.; Sun, X. M.; Li, H. P.; Peng, H. S., Stretchable, Wearable Dye-Sensitized Solar Cells. *Adv. Mater.* **2014,** *26* (17), 2643-2647.
25. Chen, T.; Qiu, L. B.; Yang, Z. B.; Cai, Z. B.; Ren, J.; Li, H. P.; Lin, H. J.; Sun, X. M.; Peng, H. S., An Integrated "Energy Wire" for both Photoelectric Conversion and Energy Storage. *Angew. Chem.-Int. Edit.* **2012,** *51* (48), 11977-11980.
26. Ali, A.; Shah, S. M.; Bozar, S.; Kazici, M.; Keskin, B.; Kaleli, M.; Akyurekli, S.; Gunes, S., Metal-free polymer/MWCNT composite fiber as an efficient counter electrode in fiber shape dye-sensitized solar cells. *Nanotechnology* **2016,** *27* (38), 10.
27. Zhang, J. X.; Wang, Z. P.; Li, X. L.; Yang, J.; Song, C. H.; Li, Y. P.; Cheng, J. L.; Guan, Q.; Wang, B., Flexible Platinum-Free Fiber-Shaped Dye Sensitized Solar Cell with 10.28% Efficiency. *ACS Appl. Energ. Mater.* **2019,** *2* (4), 2870-2877.
28. Chen, X. X.; Tang, Q. W.; He, B. L.; Lin, L.; Yu, L. M., Platinum-Free Binary Co-Ni Alloy Counter Electrodes for Efficient Dye-Sensitized Solar Cells. *Angew. Chem.-Int. Edit.* **2014,** *53* (40), 10799-10803.
29. Dinari, M.; Momeni, M. M.; Goudarzirad, M., Dye-sensitized solar cells based on nanocomposite of polyaniline/graphene quantum dots. *J. Mater. Sci.* **2016,** *51* (6), 2964-2971.
30. Zhuo, J. Q.; Caban-Acevedo, M.; Liang, H. F.; Samad, L.; Ding, Q.; Fu, Y. P.; Li, M. X.; Jin, S., High-Performance Electrocatalysis for Hydrogen Evolution Reaction Using Se-Doped Pyrite-Phase Nickel Diphosphide Nanostructures. *ACS Catal.* **2015,** *5* (11), 6355-6361.

31. Chen, H. C.; Jiang, J. J.; Zhao, Y. D.; Zhang, L.; Guo, D. Q.; Xia, D. D., One-pot synthesis of porous nickel cobalt sulphides: tuning the composition for superior pseudocapacitance. *J. Mater. Chem. A* **2015,** *3* (1), 428-437.
32. Gao, M. R.; Lin, Z. Y.; Zhuang, T. T.; Jiang, J.; Xu, Y. F.; Zheng, Y. R.; Yu, S. H., Mixed-solution synthesis of sea urchin-like NiSe nanofiber assemblies as economical Pt-free catalysts for electrochemical H-2 production. *J. Mater. Chem.* **2012,** *22* (27), 13662-13668.
33. Shao, L.; Qian, X.; Li, H. M.; Xu, C.; Hou, L. X., Shape-controllable syntheses of ternary Ni-Co-Se alloy hollow microspheres as highly efficient catalytic materials for dye-sensitized solar cells. *Chem. Eng. J.* **2017,** *315*, 562-572.
34. Chen, L.; Zhou, Y.; Dai, H.; Li, Z.; Yu, T.; Liu, J.; Zou, Z., Fiber dye-sensitized solar cells consisting of TiO 2 nanowires arrays on Ti thread as photoanodes through a low-cost, scalable route. *Journal of Materials Chemistry A* **2013,** *1* (38), 11790-11794.
35. Theerthagiri, J.; Senthil, R.; Buraidah, M.; Raghavender, M.; Madhavan, J.; Arof, A., Synthesis and characterization of (Ni1− xCox) Se2 based ternary selenides as electrocatalyst for triiodide reduction in dye-sensitized solar cells. *Journal of Solid State Chemistry* **2016,** *238*, 113-120.
36. Zhu, Y.; Ji, X.; Wu, Z.; Liu, Y., NiCo2S4 hollow microsphere decorated by acetylene black for high-performance asymmetric supercapacitor. *Electrochimica Acta* **2015,** *186*, 562-571.
37. Peng, S.; Li, L.; Tan, H.; Cai, R.; Shi, W.; Li, C.; Mhaisalkar, S. G.; Srinivasan, M.; Ramakrishna, S.; Yan, Q., MS2 (M= Co and Ni) Hollow Spheres with Tunable Interiors for High‐Performance Supercapacitors and Photovoltaics. *Advanced Functional Materials* **2014,** *24* (15), 2155-2162.
38. Shi, W.; Zhang, X.; Che, G., Hydrothermal synthesis and electrochemical hydrogen storage performance of porous hollow NiSe nanospheres. *International journal of hydrogen energy* **2013,** *38* (17), 7037-7045.
39. Shen, L.; Yu, L.; Wu, H. B.; Yu, X.-Y.; Zhang, X.; Lou, X. W. D., Formation of nickel cobalt sulfide ball-in-ball hollow spheres with enhanced electrochemical pseudocapacitive properties. *Nature communications* **2015,** *6* (1), 1-8.
40. Yu, X. L.; Cao, C. B.; Zhu, H. S.; Li, Q. S.; Liu, C. L.; Gong, Q. H., Nanometer‐Sized Copper Sulfide Hollow Spheres with Strong Optical‐Limiting Properties. *Advanced Functional Materials* **2007,** *17* (8), 1397-1401.
41. Zhang, G.; Wang, W.; Yu, Q.; Li, X., Facile one-pot synthesis of PbSe and NiSe2 hollow spheres: Kirkendall-effect-induced growth and related properties. *Chemistry of Materials* **2009,** *21* (5), 969-974.